

SHELX76 and SHELXS86.¹⁷

Acknowledgment. This work was supported by NATO International Collaborative Research Grant No. 0196/85, by the Deutsche Forschungsgemeinschaft, Grant SFB247, and by Na-

(17) Sheldrick, G. M., SHELX76 program for crystal structure determination. Cambridge, England, 1976; SHELXS86. Göttingen, FRG, 1986.

tional Science Foundation Grant No. CHE 8721657 (to R.N.G.). We thank Dr. James Davis for the unit resolution mass spectra.

Supplementary Material Available: Tables of thermal parameters and mean planes (2 pages); a table of calculated and observed structure factors (12 pages). Ordering information is given on any current masthead page.

Contribution from the Departament de Química, Universitat de les Illes Balears, Carretera de Valldemossa, km 7.5, 07071 Palma de Mallorca, Spain, Departament de Química Inorgànica, Universitat de Barcelona, Plaça Imperial Tàrraco 1, 43005 Tarragona, Spain, and Departament de Cristal·lografia, Universitat de Barcelona, Martí i Franquès s/n, 08028 Barcelona, Spain

Synthesis and Characterization of Nickel(II) Complexes of Purine and Pyrimidine Bases. Crystal and Molecular Structure of *trans*-Bis(cytosine-*O*²)bis(ethylenediamine)nickel(II) Bis(tetraphenylborate). An Unusual Metal Binding Mode of Cytosine

Gemma Cervantes,[†] Juan J. Fiol,[†] Angel Terrón,[†] Virtudes Moreno,^{*‡} Juan R. Alabart,[†] Magdalena Aguiló,[‡] Montserrat Gómez,[§] and Xavier Solans[§]

Received March 8, 1990

Three nucleobase complexes [Ni(en)₂(Ade)]Cl₂ (1), [Ni(en)₂(Hyp)]Cl·0.5CH₃OH·H₂O (2) and [Ni(en)₂(Cyt)₂][B(C₆H₅)₄]₂ (3) (en = ethylenediamine; Ade = adenine; Hyp = hypoxanthine; Cyt = cytosine) have been prepared by reaction of Ni(en)₂Cl₂ and the corresponding purine or pyrimidine base in a methanol (1, 2) or an ethanol–water (3) medium. The cytosine complex was obtained in the form of suitable crystals for X-ray crystallography. The complex crystallizes in the monoclinic space group *P*2₁/*a* with *a* = 18.985 (4) Å, *b* = 9.685 (2) Å, *c* = 16.010 (4) Å, β = 113.23 (3)°, *V* = 2705 (2), and *Z* = 2. The structure was refined by a full-matrix least-squares technique on the basis of 2090 observed reflections (*I* ≥ 2.5σ(*I*)) to a final *R* value of 0.061. Contrary to what could be expected, both unsubstituted cytosine bases are bound in the *trans* position exclusively via O(2) to the nickel atom. The octahedral coordination of Ni(II) is completed by four nitrogen atoms of two ethylenediamine molecules. Metal binding sites of the nucleobases in the three complexes are discussed in terms of their IR and electronic spectra and magnetic properties. Thermogravimetric data are in agreement with the stoichiometry and formulas proposed.

Introduction

The participation of transition-metal ions in the replication and transcription processes of DNA is well documented.¹ The influences of several divalent metal ions including Ni(II) on DNA structure unwinding and rewinding the double helix under appropriate conditions indicate that these metal ions can bind to both the bases and the phosphate groups.² Interest in the specific interactions between Ni(II) and nucleic acid constituents arises in part due to its high carcinogenicity and accumulation indices (the ratio of the amount of atoms endogenously bound with calf thymus-DNA to their concentration in mammalian serum) as compared to other essential elements.³ A considerable number of X-ray crystallographic studies on model compounds have provided information about nucleobase–metal interactions and have identified the ring nitrogen atoms as the preferred coordination sites.⁴ However, very little structural information is available regarding the binding site of Ni(II) in unsubstituted purine and pyrimidine bases⁵ and fewer studies have definitively shown direct involvement in metal binding of the exocyclic groups of these heterocycles.^{6–8} Marzilli and co-workers have evaluated the role that exocyclic groups on nucleic acid bases play in determining both the structure and stability of metal complexes.⁹ We have recently described structures of two octahedral Ni(II) ternary complexes with guanosine 5'-monophosphate and inosine 5'-monophosphate nucleotides. In both complexes, Ni(II) is surrounded by two water molecules, one ethylenediamine molecule, and two nucleotide molecules bound through N(7).¹⁰ We report here the synthesis and characterization by spectroscopic methods of three nickel(II) nucleobase ternary complexes and the structural properties of the unusual cytosine complex. This is the first

crystallographic evidence of monodentate O(2) binding in neutral unsubstituted cytosine.

Experimental Section

Analyses and Physical Measurements. Analytical results were carried out in a Carlo Erba model 1106 microanalyzer (Centro de Investigación y Desarrollo-CSIC, Depto. Q.O.B., Barcelona, Spain). Nickel content was determined by atomic absorption in a Perkin-Elmer 703 spectrophotometer. The infrared spectra were registered in the solid state (KBr pellets) on a PE 683 instrument with a PE 1600 infrared data station,

- (1) (a) Martin, R. B.; Mariam, Y. H. *Met. Ions Biol. Syst.* **1979**, *8*, 57–124. (b) Spiro, T. G., Ed. *Nucleic Acid-Metal Ion Interactions*; Wiley: New York, 1980; Vol. 1. (c) Marzilli, L. G. *Prog. Inorg. Chem.* **1977**, *23*, 255–378. (d) Hodgson, D. J. *Prog. Inorg. Chem.* **1977**, *23*, 211–254. (e) Eichhorn, G. L. In *Inorganic Biochemistry*; Eichhorn, G. L., Ed.; Elsevier: Amsterdam, 1973; Vol. 2, Chapters 33 and 34.
- (2) Eichhorn, G. L. *J. Am. Chem. Soc.* **1968**, *90*, 7323.
- (3) Andronikashvili, E. L.; Bregadze, V. G.; Monaselidze, J. R. *Met. Ions Biol. Syst.* **1988**, *23*, 331–357.
- (4) (a) Swaminathan, V.; Sundaralingam, M. *CRC Crit. Rev. Biochem.* **1979**, *6*, 245–336. (b) Aoki, K. *Nippon Kessho Gakkarischi* **1981**, *23*, 309–327. (c) Pezzano, H.; Podo, F. *Chem. Rev.* **1980**, *80*, 365–401.
- (5) Dubler, E.; Hanggi, G.; Bensch, W. J. *J. Inorg. Biochem.* **1987**, *29*, 269.
- (6) (a) Marzilli, L. G.; Kistenmacher, T. J.; Rossi, M. J. *Am. Chem. Soc.* **1977**, *99*, 2797. (b) Beyerle-Pfnur, R.; Shollhorn, H.; Thewalt, U.; Lippert, B. *J. Chem. Soc., Chem. Commun.* **1985**, 1510–1511. (c) Aoki, K. *J. Chem. Soc., Chem. Commun.* **1976**, 748–749.
- (7) (a) Charland, J. P.; Beauchamp, A. L. *Inorg. Chem.* **1986**, *25*, 4870. (b) Prizant, L.; Olivier, M. J.; Rivest, R.; Beauchamp, A. L. *J. Am. Chem. Soc.* **1979**, *101*, 2765. (c) Charland, J. P. *Inorg. Chim. Acta* **1987**, *135*, 191.
- (8) (a) Guay, F.; Beauchamp, A. L. *J. Am. Chem. Soc.* **1979**, *101*, 6260. (b) Cartwright, B. A.; Goodgame, M.; Johns, K. W.; Skapski, A. C. *Biochem. J.* **1978**, *175*, 337. (c) Schollhorn, H.; Eisenmann, P.; Thewalt, U.; Lippert, B. *Inorg. Chem.* **1986**, *25*, 3384.
- (9) (a) Marzilli, L. G.; Kistenmacher, T. J. *Acc. Chem. Res.* **1977**, *10*, 146. (b) Marzilli, L. G.; Steward, R. C.; Van Vuuren, C. P.; Castro, B.; Caradona, J. R. *J. Am. Chem. Soc.* **1978**, *100*, 3967. (c) Kistenmacher, T. J.; Rossi, M.; Marzilli, L. G. *Inorg. Chem.* **1979**, *18*, 240. (d) Szalda, D. J.; Kistenmacher, T. J.; Marzilli, L. G. *J. Am. Chem. Soc.* **1976**, *98*, 8371.
- (10) Fiol, J. J.; Terrón, A.; Calafat, A. M.; Moreno, V.; Aguiló, M.; Solans, X. *J. Inorg. Biochem.* **1989**, *35*, 191.

[†] Universitat Illes Balears.

[‡] Departament de Química, Universitat de Barcelona.

[§] Departament de Cristal·lografia, Universitat de Barcelona.

and the electronic spectra were registered on a PE 552 spectrophotometer. Thermogravimetric data in the temperature range from 30 to 930 °C were recorded in a flowing-air atmosphere (heating rate 5 °C/min) on a PE TGA-2 thermobalance. Magnetic susceptibility measurements in the 14–300 K temperature range were carried out on powdered samples on a Faraday-type microbalance calibrated with $\text{Hg}[\text{Co}(\text{NCS})_4]^{11}$ at a magnetic field of ca. 0.25 T, at the Departament de Física Fonamental, Barcelona, Spain. Magnetic susceptibilities below 14 K were obtained by using a SHE SQUID type susceptometer at 1 and 0.5 T for the hypoxanthine and the adenine derivatives respectively, at the Departament de Física Fonamental. Diamagnetic corrections of -457×10^{-6} (3), -190×10^{-6} (1), and $-184 \times 10^{-6} \text{ cm}^3 \text{ mol}^{-1}$ (2), calculated from Pascal's constants, were applied.¹² Experimental magnetic susceptibilities were fit to theoretical expressions with a local computer routine that employs one minimization NAG FORTRAN subroutine.¹³ Crystallographic studies were performed on a Philips PW-1100 four-circle diffractometer. Adenine, hypoxanthine, and cytosine were obtained from Merck and used without further purification. The starting complex $[\text{Ni}(\text{en})_2\text{Cl}]_2\text{Cl}_2$ was prepared by the method described in the literature.¹⁴

Preparative Method. (a) $[\text{Ni}(\text{en})_2(\text{Ade})]\text{Cl}_2$. A 2-mmol sample of adenine was dissolved in 90 mL of hot methanol, and the resulting solution was added to a stirred, hot solution of 2 mmol of $\text{Ni}(\text{en})_2\text{Cl}_2$ in 25 mL of methanol. The mixture was boiled under reflux for 18 h and then rotaevaporated at 50 °C and boiled again under reflux for 1 h. The blue precipitate obtained was washed with methanol and air-dried. The product is slightly soluble in water and methanol. Thermal analysis of the title complex shows that the compound is thermally stable up to 260 °C. The subsequent decomposition up to 900 °C finally leads to NiO in good agreement with the corresponding observed weight loss. Anal. Calcd for $\text{C}_9\text{H}_{21}\text{N}_9\text{Cl}_2\text{Ni}$: C, 28.08; H, 5.50; N, 32.75; Ni, 15.25; Cl, 18.42. Found: C, 27.57; H, 5.47; N, 32.43; Ni, 14.70; Cl, 18.29. IR (cm^{-1}): 319 w, 338 w, 420 w, 444 w, 509 m, 524 m, 535 m, 567 m, 609 m, 622 m, 657 m, 687 m, 724 m, 765 w, 799 m, 900 m, 943 vw, 1022 vs, 1103 m, 1131 w, 1229 m, 1252 m, 1277 m, 1311 m, 1330 m, 1356 m, 1395 s, 1453 s, 1481 m, 1502 m, 1564 s, 1579 m, 1607 s, 1649 vs. Δ_M ($\Omega^{-1} \text{ cm}^2 \text{ mol}^{-1}$) of 10^{-3} M in H_2O at 20 °C = 260.

(b) $[\text{Ni}(\text{en})_2(\text{Hyp})\text{Cl} \cdot 0.5\text{CH}_3\text{OH} \cdot \text{H}_2\text{O}]$. To a hot solution of 1 mmol of $\text{Ni}(\text{en})_2\text{Cl}_2$ in 15 mL of methanol was added 1 mmol of hypoxanthine in 30 mL of methanol and 10 mL of a 0.1 mol/L tetra-*n*-butylammonium hydroxide solution in 2-propanol–methanol (Merck). The violet solution was boiled under reflux for 4 h. After 1 day, the violet solid obtained was washed with methanol and dried under vacuum. The product is slightly soluble in water and methanol. The complex exhibits a weight loss between 40 and 120 °C attributable to the elimination of one methanol molecule and two water molecules per two formula units (mass loss calcd, 8.86%; mass loss found, 8.32%). The subsequent decomposition occurs between 200 and about 600 °C and finally leads to NiO. Anal. Calcd for $\text{C}_9\text{H}_{19}\text{N}_8\text{OClNi} \cdot 0.5\text{CH}_3\text{OH} \cdot \text{H}_2\text{O}$: C, 29.75; H, 6.05; N, 29.22; Ni, 15.31; Cl, 9.24. Found: C, 29.80; H, 5.92; N, 29.05; Ni, 15.00; Cl, 9.35. IR (cm^{-1}): 326 vw, 375 w, 517 w, 575 w, 622 m, 661 m, 715 w, 793 m, 909 w, 976 m, 1022 vs, 1099 m, 1146 w, 1190 s, 1202 s, 1274 w, 1279 m, 1339 m, 1370 sh, 1388 s, 1432 w, 1458 w, 1492 w, 1511 w, 1588 vs, 1670 vs. Δ_M ($\Omega^{-1} \text{ cm}^2 \text{ mol}^{-1}$) of 10^{-3} M in MeOH at 20 °C = 91.3.

(c) $[\text{Ni}(\text{en})_2(\text{Cyt})_2\text{IB}(\text{C}_6\text{H}_5)_2]_2$. To a hot solution (70 °C) of 0.5 mmol of $\text{Ni}(\text{en})_2\text{Cl}_2$ in 10 mL of a 9:1 v/v mixture of ethanol–water was added an equimolar amount of the appropriate ligand suspended in 5 mL of a 4:1 v/v mixture of ethanol–water. The deep blue mixture was heated for about 1 h on a steam bath (80 °C); a light blue solution was the result. A hot solution (80 °C) of NaBPh_4 (1 mmol) in 5 mL of a 4:1 v/v mixture of ethanol–water was then added, and the resultant mixture was filtered off. After 3 days, pink-purple hexagonal crystals of the cytosine complex could be isolated, washed with ethanol, and air-dried. Deep purple rhomboidal crystals of the same complex were obtained afterward by the same method, but cold solutions of cytosine and NaBPh_4 were added. No color change was observed in this case after the adding of ligand. The complex is thermally stable up to 190 °C. At this point it exhibits a weight loss up to 290 °C corresponding to the loss of the eight phenyl groups per formula unit (mass loss calcd, 59.29%; mass loss found, 59.02%). Two additional step reactions (290–790 °C) are identified with the loss of two cytosine and two ethylenediamine molecules respectively per formula unit (mass loss calcd, 21.39%, 11.56%; mass loss found, 20.83%, 12.40%). A mixture of NiO and B_2O_3 is identified as the final residue. Anal. Calcd for $\text{C}_{60}\text{H}_{66}\text{N}_{10}\text{O}_2\text{B}_2\text{Ni}$: C, 69.32; H, 6.40; N,

Table I. Crystal Data and Structure Solution Parameters for $[\text{Ni}(\text{en})_2(\text{Cyt})_2][\text{B}(\text{C}_6\text{H}_5)_2]_2$

formula (fw)	$\text{C}_{60}\text{H}_{66}\text{N}_{10}\text{O}_2\text{B}_2\text{Ni}$ (1039.6)
cryst syst	monoclinic
space group	$P2_1/a$
<i>a</i> , Å	18.985 (4)
<i>b</i> , Å	9.685 (2)
<i>c</i> , Å	16.010 (4)
β , deg	113.23 (3)
<i>V</i> , Å ³	2705 (2)
<i>Z</i>	2
<i>F</i> (000)	1100
<i>D_c</i> g/cm ³	1.273
cryst form and size	tabular (0.1 × 0.1 × 0.08)
μ , cm ⁻¹	4.16
radiation (λ , Å)	Mo K α (0.71069)
scan method	ω scan
data colln range (θ), deg	2–25
data collcd	$\pm h, +k, +l$
syst abs	(<i>h</i> 0 <i>l</i>) <i>h</i> = 2 <i>n</i> + 1 (0 <i>k</i> 0) <i>k</i> = 2 <i>n</i> + 1
<i>R</i> _{int} (on <i>F</i>)	0.24
no. of reflns measd	3456
no. of reflns obsd (<i>I</i> ≥ 2.5 σ (<i>I</i>))	2090
no. of variables	440
<i>R</i>	0.061
<i>R_w</i>	0.066
weighting scheme <i>K</i> , ($\sigma^2(F_o) + K(F_o)^2$) ⁻¹	0.016

13.47; Ni, 5.65. Found: C, 69.40; H, 6.44; N, 13.23; Ni, 5.50. IR (cm^{-1}): 311 w, 383 w, 425 m, 445 m, 494 w, 517 m, 564 m, 596 m, 612 s, 659 s, 709 s, 734 s, 747 s, 785 m, 807 m, 843 sh, 854 m, 919 w, 964 m, 1102 s, 1032 m, 1068 w, 1101 m, 1126 m, 1143 m, 1187 w, 1205 s, 1267 w, 1291 m, 1356 m, 1416 m, 1428 m, 1450 sh, 1487 s, 1525 m, 1601 vs, 1633 vs, 1646 vs, 1760 w, 1840 w, 1892 w, 1955 w. Δ_M ($\Omega^{-1} \text{ cm}^2 \text{ mol}^{-1}$) of 10^{-3} M in MeOH at 20 °C = 158.7.

Crystallographic Studies. A tabular crystal (0.1 × 0.1 × 0.08 mm) was selected and mounted on a Phillips PW-1100 four-circle diffractometer. Unit cell parameters were determined from 25 reflections ($4 \leq \theta \leq 12^\circ$) and refined by a least-squares method. Intensities were collected with graphite monochromatized Mo K α radiation by using the ω -scan technique, scan width 0.8°, and scan speed 0.03° s⁻¹. A total of 3456 reflections were measured in the range $2 \leq \theta \leq 25^\circ$. Three reflections were measured every 2 h as orientation and intensity control. Significant intensity decay was not observed. The set of 2090 with $I \geq 2.5\sigma(I)$ was used in the subsequent calculations. *R*_{int} for equivalent reflections was 0.24. Lorentz polarization but no absorption corrections were made. The structure was resolved by direct methods, using the MULTAN system of computer programs,¹⁵ and refined by a full-matrix least-squares method, using the SHELX76 computer program.¹⁶ The function minimized was $\sum w[|F_o| - |F_c|]^2$, where $w = [\sigma^2(F_o) + 0.016(F_o)^2]^{-1}$ and f, f', f'' were taken from ref 17. The positions of eight H atoms were computed, and the remaining atoms were located from a difference synthesis. All of them were refined with an overall isotropic temperature factor using a riding model for computed hydrogen atoms, while the remaining non-hydrogen atoms were refined anisotropically. The final *R* factor was 0.061 (*R_w* = 0.066) for all observed reflections. The number of refined parameters was 440. The maximum shift/esd was 0.2 in *y* of C(23); maximum and minimum peaks in the final difference synthesis were 0.4 and -0.3 Å⁻³ respectively. Crystal parameters, data collection details, and results of the refinements are summarized in Table I.

Results and Discussion

Results of single-crystal X-ray diffraction studies of cytosine, cytidine, and cytidine 5'-monophosphate complexes have shown that N(3),¹⁸ chelation N(3)–O(2),¹⁹ bridging N(3)–O(2),^{9c} and

- (11) Bunzli, J. C. G. *Inorg. Chim. Acta* **1979**, *36*, L413.
 (12) Mabbs, F. E.; Machin, D. J. *Magnetism and Transition Metal Complexes*; Chapman and Hall: London, 1973.
 (13) NAG Fortran Library Mark 12.
 (14) State, H. M. *Inorg. Synth.* **1960**, *6*, 198.

- (15) Main, P.; Fiske, S. E.; Hull, S. L.; Lessinger, L.; Germain, G.; Declercq, J. P.; Woolson, M. MULTAN, an Automatic System of Computer Programs for Crystal Structure Determination from X-Ray Diffraction Data. Universities of York, U.K., and Louvain, Belgium, 1984.
 (16) Sheldrick, G. M. SHELX 76. A Computer Program for Crystal Structure Determination. University of Cambridge, U.K., 1976.
 (17) *International Tables for X-Ray Crystallography*; Kynoch Press: Birmingham, England; 1974; Vol. 4, pp 99–100 and 149.
 (18) (a) Sinn, E.; Flynn, C. M.; Martin, R. B. *Inorg. Chem.* **1977**, *16*, 2403. (b) Miller, S. K.; Marzilli, L. G.; Dorre, S.; Kollat, P.; Stigler, R. G.; Stezowski, J. J. *Inorg. Chem.* **1986**, *25*, 4272. (c) Goodgame, D. M. L.; Jeeves, I.; Reynolds, C. D.; Skapski, A. C. *Biochem. J.* **1975**, *151*, 467. (d) Clark, G. R.; Orbell, J. D. *Acta Cryst.* **1978**, *B34*, 1815. (e) Beauchamp, A. L. *Inorg. Chim. Acta* **1984**, *91*, 33.
 (19) (a) Shiba, J. K.; Bau, R. *Inorg. Chem.* **1978**, *17*, 3484. (b) Aoki, K.; Saenger, W. J. *Inorg. Biochem.* **1984**, *20*, 225.

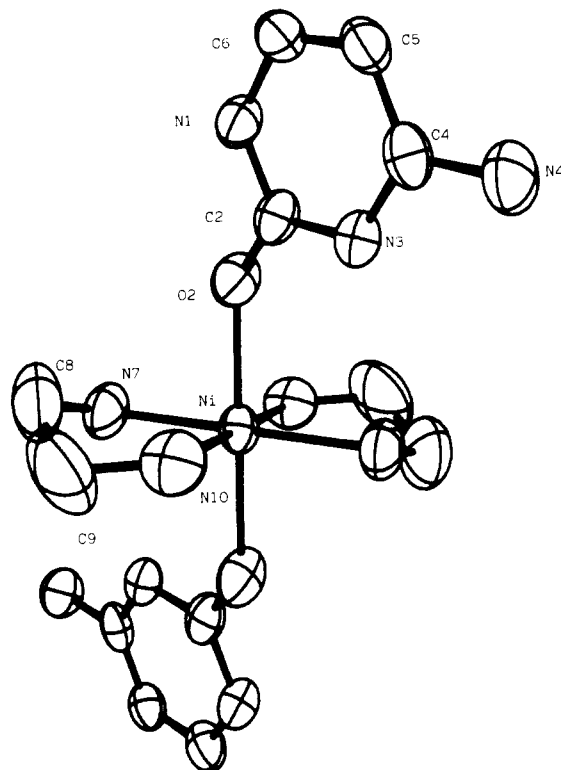


Figure 1. Structure of $[\text{Ni}(\text{en})_2(\text{Cyt})_2]^{2+}$ (cation of **3**) showing 50% probability thermal ellipsoids (hydrogen atoms are omitted for clarity).

N(3)—additional O(2) weak interaction²⁰ are the preferred binding modes for transition-metal ions. Three modes of metal coordination to anionic cytosine residues (deprotonated at the exocyclic amino group N(4)) have been reported: monodentate N(4) binding,²¹ chelation N(3)—N(4),^{6c} and bridging N(3)—N(4).²² Although theoretical²³ and ¹³C NMR—Raman spectroscopic studies^{9b,24} strongly suggest that monofunctional exocyclic O(2) binding is possible, only one crystallographic piece of evidence has been reported to date.^{6b} In the octahedral complex $\text{Mn}(5'-\text{CMP}) \cdot 2.5\text{H}_2\text{O}$, it was found that manganese forms a strong bond (2.08 Å) with the O(2) of the pyrimidine ring. The coordination about the Mn(II) is completed by a water molecule and four oxygen atoms of three different phosphate groups. It has been suggested that the O(2) binding mode may be the result of minimal steric requirements^{24a} and does not seem to be strongly affected by the hard/soft nature of the metal ion. In the polymeric silver(I) complex of 1-methylcytosine $[\text{Ag}(\text{C}_5\text{H}_7\text{N}_3\text{O})(\text{NO}_3)]_n$, the Ag(I), which normally prefers soft donors, binds to the exocyclic O(2) $[\text{Ag}-\text{O}(2) = 2.367(2) \text{ \AA}]$.^{9c} In other chelate N(3)—O(2) complexes¹⁹ of Cd(II) and 5'-CMP the metal—O(2) interactions are substantially weaker, ranging from 2.58 to 2.87 Å. The cytosine complex (**3**) reported here does not fit the general coordination pattern exhibited by other known cytosine complexes. The Ni(II) ion, of intermediate hard/soft nature, binds strongly to the exocyclic O(2) $[\text{Ni}-\text{O}(2) = 2.128(3) \text{ \AA}]$ as in the case of the Mn—5'-CMP complex.

Table II. Final Atomic Coordinates ($\times 10^4$) for Non-Hydrogen Atoms of **3**

	<i>x/a</i>	<i>y/b</i>	<i>z/c</i>	$B_{\text{eq}}, \text{ \AA}^2$
Ni	0	5000	0	3.14 (7)
N(1)	-464 (4)	5643 (7)	2414 (4)	3.8 (3)
C(2)	-18 (5)	5619 (8)	1910 (6)	3.5 (4)
O(2)	-365 (3)	5527 (6)	1057 (4)	4.4 (3)
N(3)	749 (3)	5665 (7)	2326 (4)	3.4 (3)
C(4)	1063 (5)	5765 (8)	3239 (6)	3.7 (4)
N(4)	1835 (4)	5855 (9)	3643 (5)	5.1 (4)
C(5)	615 (5)	5784 (9)	3772 (6)	3.7 (4)
C(6)	-146 (5)	5742 (9)	3342 (6)	4.0 (4)
N(7)	1076 (4)	5915 (9)	600 (5)	5.0 (4)
C(8)	1039 (8)	7258 (14)	137 (11)	8.8 (9)
C(9)	300 (9)	7892 (13)	-104 (10)	9.5 (9)
N(10)	-335 (5)	6950 (8)	-552 (5)	5.1 (4)
B	2421 (5)	915 (9)	2823 (6)	2.7 (4)
C(11)	2326 (4)	1551 (8)	1822 (5)	3.0 (3)
C(12)	2646 (5)	2761 (10)	1678 (6)	4.2 (5)
C(13)	2515 (6)	3258 (12)	798 (8)	5.4 (6)
C(14)	2049 (6)	2558 (14)	44 (8)	5.7 (6)
C(15)	1707 (6)	1339 (12)	147 (6)	5.2 (5)
C(16)	1836 (5)	862 (9)	1033 (5)	3.9 (4)
C(17)	1541 (4)	806 (8)	2787 (4)	2.8 (3)
C(18)	1148 (5)	-435 (9)	2656 (5)	3.6 (4)
C(19)	367 (5)	-509 (10)	2535 (6)	4.4 (5)
C(20)	-28 (5)	678 (11)	2563 (6)	4.2 (4)
C(21)	357 (5)	1938 (10)	2695 (6)	4.2 (4)
C(22)	1122 (5)	1984 (9)	2790 (5)	3.2 (4)
C(23)	2821 (4)	-641 (8)	2007 (5)	2.7 (3)
C(24)	2859 (4)	-1530 (9)	2349 (6)	3.4 (4)
C(25)	3175 (5)	-2849 (9)	2525 (6)	4.2 (4)
C(26)	3492 (5)	-3310 (10)	3435 (7)	4.7 (5)
C(27)	3456 (5)	-2465 (9)	4113 (6)	3.9 (4)
C(28)	3121 (4)	-1172 (8)	3893 (5)	3.1 (4)
C(29)	2994 (4)	1935 (7)	3639 (5)	2.8 (3)
C(30)	2802 (4)	2641 (8)	4285 (5)	3.3 (4)
C(31)	3323 (6)	3510 (9)	4945 (6)	4.4 (5)
C(32)	4063 (6)	3693 (10)	4983 (6)	4.5 (5)
C(33)	4274 (5)	3004 (9)	4365 (6)	4.1 (5)
C(34)	3747 (5)	2143 (9)	3710 (5)	3.5 (4)

$$^a B_{\text{eq}} = (8\pi^2/3) \sum U_{ij} a_i^* a_j^* a_i a_j$$

Table III. Interatomic Bond Lengths (Å) and Angles (deg) for **3**

O(2)—Ni	2.128 (3)	C(4)—N(3)	1.347 (6)
N(7)—Ni	2.081 (4)	C(4)—N(4)	1.353 (6)
N(10)—Ni	2.076 (4)	C(4)—C(5)	1.422 (7)
N(1)—C(2)	1.381 (6)	C(6)—C(5)	1.334 (7)
N(1)—C(6)	1.369 (6)	C(8)—N(7)	1.486 (9)
C(2)—O(2)	1.263 (5)	C(9)—C(8)	1.437 (10)
N(3)—C(2)	1.342 (6)	N(10)—C(9)	1.456 (9)
N(7)—Ni—O(2)	95.6 (8)	C(5)—C(4)—N(3)	122.6 (4)
N(10)—Ni—O(2)	88.8 (2)	N(4)—C(4)—N(3)	117.1 (5)
N(10)—Ni—N(7)	83.7 (2)	N(4)—C(4)—C(5)	120.3 (5)
C(6)—N(1)—C(2)	121.7 (3)	C(6)—C(5)—C(4)	118.1 (5)
C(2)—O(2)—Ni	133.0 (3)	N(1)—C(6)—C(5)	119.2 (5)
N(3)—C(2)—O(2)	122.7 (4)	C(8)—N(7)—Ni	107.3 (4)
N(1)—C(2)—O(2)	117.0 (4)	C(9)—C(8)—N(7)	110.9 (6)
N(1)—C(2)—N(3)	120.3 (5)	N(10)—C(9)—C(8)	113.3 (6)
C(4)—N(3)—C(2)	118.0 (4)	C(9)—N(10)—Ni	107.7 (4)

Description of the Structure of 3. The molecular structure of $[\text{Ni}(\text{en})_2(\text{Cyt})_2][\text{B}(\text{C}_6\text{H}_5)_4]_2$ (**3**) together with the crystallographic atomic numbering scheme is shown in Figure 1.

The final non-hydrogen atomic coordinates and equivalent thermal coefficients are listed in Table II. Selected bond distances and bond angles are given in Table III.

Final hydrogen coordinates, anisotropic thermal parameters of atoms, and other interatomic bond lengths and angles are contained in the supplementary material.

In the structure, the Ni(II) ion lies on a crystallographic inversion center and exhibits octahedral coordination by four nitrogen atoms of two ethylenediamine ligands in the basal plane $[\text{Ni}-\text{N}(\text{en})_{\text{av}} = 2.078 \text{ \AA}]$ and two exocyclic O(2) atoms of two cytosine bases in the axial positions $[\text{Ni}-\text{O}(2) = 2.128(3) \text{ \AA}]$. In addition, the Ni(II) lies on an inversion center, which is at the

- (20) (a) Szalda, D. J.; Marzilli, L. G.; Kistenmacher, T. J. *Biochem. Biophys. Res. Commun.* **1975**, *63*, 601. (b) Aoki, K. *Biochim. Biophys. Acta* **1976**, *447*, 379. (c) Kistenmacher, T. J.; Szalda, D. J.; Marzilli, L. G. *Acta Crystallogr.* **1975**, *B31*, 2416. (d) Sundaralingam, M.; Carrabine, J. A. *J. Mol. Biol.* **1971**, *61*, 287. (e) Szalda, D. J.; Marzilli, L. G.; Kistenmacher, T. J. *Inorg. Chem.* **1975**, *14*, 2076.
- (21) (a) Clarke, M. J. *J. Am. Chem. Soc.* **1978**, *100*, 5068. (b) Graves, B. J.; Hodgson, D. J. *J. Am. Chem. Soc.* **1979**, *101*, 5608.
- (22) Faggiani, R.; Lippert, B.; Lock, C. J. L.; Speranzini, R. A. *J. Am. Chem. Soc.* **1981**, *103*, 1111.
- (23) Bonaccorsi, R.; Pullman, A.; Scrocco, E.; Tomasi, J. *Theor. Chim. Acta* **1972**, *24*, 51.
- (24) (a) Kozlowski, H.; Matczak-Jon, E. *Pol. J. Chem.* **1981**, *55*, 2243. (b) Marzilli, L. G.; Castro, B.; Caradona, J. P.; Stewart, R. C.; Van Vuuren, C. P. *J. Am. Chem. Soc.* **1980**, *102*, 916.

Table IV. Characteristic IR Bands for the Complexes and Free Ligands (cm⁻¹)

band assign ^a	Ade	1	Hyp	2	Cyt	3
$\nu(\text{N}(9)-\text{H})$	2800–2500 s, br					
$\delta(\text{NH}_2) + \nu(\text{C}(5)-\text{C}(6)) + \nu(\text{C}(6)-\text{NH}_2)$	1674 vs	1649 vs				
$\nu(\text{C}(6)=\text{O})$			1672 s	1670 s		
$\nu(\text{C}(2)=\text{O})$					1664 vs	1646 vs
$\nu(\text{C}=\text{C}) + \nu(\text{C}=\text{N}) + \delta(\text{NH}_2)$		1564 s ^b			1636, 1617 s	1636, 1601 vs
$\nu(\text{C}(4)-\text{N}(9)) + \delta(\text{C}(8)-\text{H})$	1508, 1471 w	1502, 1481 m				
$\nu(\text{ring})$					1504, 1466 s, 1366 s	1487 vs, 1450 sh,m 1356 s
$\nu(\text{C}(8)=\text{N}(7)) + \delta(\text{C}(8)-\text{H})$			1469 s	1458 w		
$\nu(\text{C}(4)-\text{N}(9)) + \nu(\text{N}(7)-\text{C}(5))$			1421 s	1432 w		
$\nu(\text{N}(1)-\text{C}(6)-\text{N}(6))$	1420 s	1395 s				
$\nu(\text{N}(9)-\text{C}(8)) + \delta(\text{C}(8)-\text{H})$			1367, 1350 s	1388, 1339 m		
$\nu(\text{ring})$	1370 m, 1337 s	1356 m, 1330 m				
$\nu(\text{N}(9)-\text{C}(8)) + \nu(\text{N}(3)=\text{C}(2)) + \delta(\text{C}-\text{H})$	1312 s	1311 w				
$\delta(\text{NH}_2) + \delta(\text{C}-\text{H}) + \nu(\text{ring})$					1279, 1238 s	1291 s, 1267 m
$\nu(\text{N}(7)-\text{C}(5)) + \nu(\text{C}(6)-\text{N}(1))$			1275 s	1279 m		
$\delta(\text{N}(9)-\text{H}) + \delta(\text{N}(7)-\text{C}(8)-\text{N}(9))$	1254 s	1252, 1229 m				
$\delta(\text{C}(8)-\text{H}) + \nu(\text{C}(8)=\text{N}(7))$			1215 s	1202, 1190 s		
$\nu(\text{C}-\text{N}) + \nu(\text{C}-\text{C})$ (en)		1020 s, br		1022 s, br		1002 s
$\delta(\text{N}(1)-\text{C}(2)-\text{N}(3)) + \nu(\text{C}(5)-\text{N}(7)) + \gamma(\text{N}(9)-\text{H})$	873 w					
$\nu(\text{Ni}-\text{N})$		338, 319 w		375, 326 w		383, 311 w

^aFree Ade band assignments based on refs 25, 26 and 29. Free Hyp band on refs 25 and 30. Free Cyt band on refs 25 and 28. ^b $\nu(\text{N}(3)-\text{C}(4)-\text{C}(5))$.
^cAbbreviations: s, strong; v, very; m, medium; sh, shoulder; w, weak; ν , stretching; δ , bending; γ , wagging.

same time a center of crystallographic symmetry. A slight distortion of the octahedral environment of nickel is indicated by the observed bond angles, which are around 90°, varying between 83.7 (2) and 95.6 (1)°. In contrast with most crystallographic reports, the present structure does not show any intramolecular hydrogen bonding. Moreover, intermolecular hydrogen bonds involving the exocyclic NH₂ group and base stacking interactions are excluded since the complex consists of monomeric molecules that are well separated due to the disposition of the BPh₄ groups between them. The unit cell of the structure is shown in Figure 2.

The bond lengths in the pyrimidine ring vary from 1.334 (7) to 1.422 (7) Å, and the angles are all close to 120°. They are similar to those found in cytosine rings of other structural studies.

Infrared Data. The infrared spectra of the obtained compounds were recorded down to the far-IR region of 200 cm⁻¹ and compared with those of the ligands. Tentative band assignments (cm⁻¹) for cytosine, adenine, and hypoxanthine according to the literature^{25–30} and some characteristic changes in the complex bands are shown in Table IV.

In the spectra of the purine complexes 1 and 2, the most noticeable changes in frequency and intensity are observed on the bands related to the imidazole ring stretching (see Figure 3). For the adenine complex the peaks appearing at 1508 and 1471 cm⁻¹ assigned to $\nu(\text{C}(4)-\text{N}(9)) + \delta(\text{C}-\text{H})$ ^{29a} increase their relative intensity, the latter shifting the frequency to 1481 cm⁻¹. This modification has been related to the N(9)–metalated ring^{29b} as well as the shift to lower frequencies by about 25 cm⁻¹ in the 1420-cm⁻¹ band involving the stretching of the N(1)–C(6) and C(6)–NH₂ bonds.^{29a} The strong band at 1674 cm⁻¹ corresponding

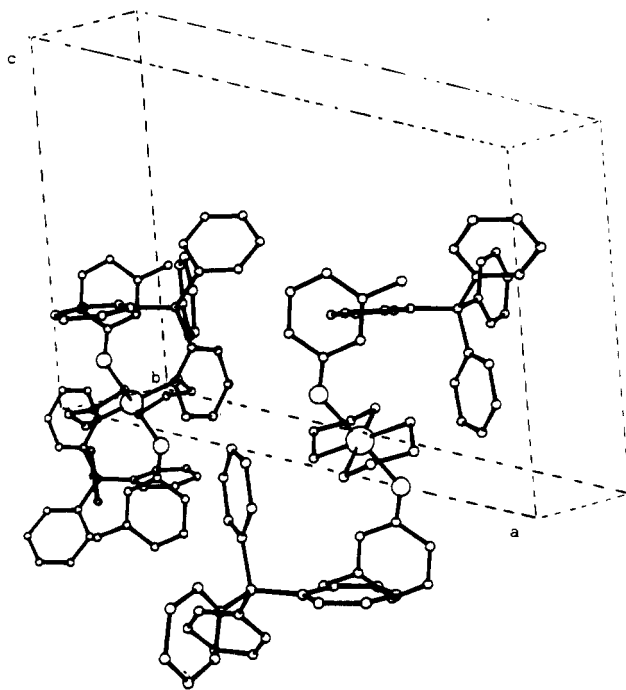


Figure 2. Drawing of the unit cell of 3.

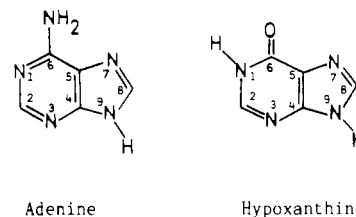


Figure 3. Chemical numbering schemes for the two purine nucleobases.

to $\delta(\text{NH}_2)$ in the free adenine is displaced to a lower frequency, 1649 cm⁻¹, as also occurs in several adenine complexes upon N(9) coordination. On the other hand, a displacement to higher frequencies in the $\delta(\text{NH}_2)$ band is interpreted by several authors^{29,31}

- (25) Tsuboi, M.; Takahashi, S.; Harada, I. In *Physicochemical Properties of Nucleic Acids*; Duchesne, J., Ed.; Academic Press: London, 1973; Vol. 2, p 91.
 (26) Tsuboi, M. in *Basic Principles in Nucleic Acid Chemistry*; Ts'o, P. O. P., Ed.; Academic Press: New York, 1974; Vol. 1, p 400.
 (27) Susi, H.; Ard, J. S.; Purcell, J. M. *Spectrochim. Acta* **1973**, *29A*, 725.
 (28) Beetz, C. P.; Ascarelli, G. *Spectrochim. Acta* **1980**, *36A*, 299.
 (29) Savoie, R.; Jutier, J. J.; Prizant, L.; Beauchamp, A. L. *Spectrochim. Acta* **1982**, *38A*, 561. (b) Prizant, L.; Olivier, M. J.; Rivest, R.; Beauchamp, A. L. *Can. J. Chem.* **1981**, *59*, 1311.
 (30) (a) Tajmir-Riahi, H. A.; Theophanides, T. *Can. J. Chem.* **1983**, *61*, 1813. (b) Mikulski, C. M.; Grossman, S.; Bayne, M. L.; Gaul, M.; Staley, D. L.; Renn, A.; Karayannis, N. M. *Inorg. Chim. Acta* **1989**, *161*, 29. (c) Mulet, D.; Calafat, A. M.; Fiol, J. J.; Terrón, A.; Moreno, V. *Inorg. Chim. Acta* **1987**, *138*, 199. (d) Tajmir-Riahi, H. A.; Theophanides, T. *Can. J. Chem.* **1984**, *62*, 1429. (e) Tajmir-Riahi, H. A.; Theophanides, T. *Can. J. Chem.* **1985**, *63*, 2085.

- (31) (a) Fujita, T.; Sakaguchi, T. *Chem. Pharm. Bull.* **1977**, *25*, 2419. (b) Shirotake, S. *Chem. Pharm. Bull.* **1980**, *28*, 1673.

Table V. Electronic Spectral Data for the Complexes (nm) with ϵ in parentheses ($\text{mol}^{-1} \text{cm}^{-1}$)

compd	$\pi \rightarrow \pi^*$	$\nu_3: {}^3A_{2g}(F) \rightarrow {}^3T_{1g}(P)$	$\nu_2: {}^3A_{2g}(F) \rightarrow {}^3T_{1g}(F)$	$10Dq, \text{cm}^{-1}$	
Ade ^a	205 (3.3×10^4) 260 (1.3×10^4)				
1 ^a	206 (8.3×10^4) 260 (5.0×10^4)	355 (19.0) 396 (14.0)	465 (6.6) 495 (6.6)	550 (10.1) 575 (10.6)	11 382
Hyp ^b	204 (1.6×10^5) 249 (2.0×10^4)				
2 ^b	209 (1.2×10^4) 255 (9.3×10^3)	347 (81)	405 (59)	545 (46)	11 900
Cyt ^b	206 (2.0×10^4) 267 (8.0×10^3)				
3 ^b	205 (1.3×10^5) 265 (1.2×10^4)	356 (18.2)	406 (8.7) 458 (5.4)	570 (10.0), 750 (5.0)	11 038

^a Aqueous solution electronic spectrum. ^b In MeOH.

as the result of N(1) protonation or metalation and the disappearance of the band is related to the substitution of an amino proton by a metal ion. Other characteristic spectral changes associated with N(9) coordination in adenine complexes described previously are observed in the spectrum of **1**: the disappearance of the three peaks assigned to $\nu(\text{N}(9)\text{--H})$ in the region 2500–2800 cm^{-1} ; the disappearance of the 873- cm^{-1} peak related to the N(9)–H out of the plane wagging mode and the splitting and decrease of the relative intensity in the 1254- cm^{-1} band assigned to the imidazole N–H rocking mode.³² All this suggests N(9)–Ni(II) binding in complex **1**. On the other hand, the modification of the band at 1337 cm^{-1} related to $\nu(\text{C}(5)\text{--N}(7)\text{--C}(8))$ and the appearance of a new band at 1564 cm^{-1} assignable to $\nu(\text{N}(3)\text{--C}(4)\text{--C}(5))$ suggest that N(3) or N(7) might be involved in coordination as well. Several X-ray crystallographic studies on adenine compounds have identified the bridging N(3)–N(9) and N(7)–N(9) as effective binding modes.^{33,34}

In the case of the hypoxanthine complex **2**, the band corresponding to $\nu(\text{C}(6)\text{=O})$, which appears around 1670 cm^{-1} , is not appreciably modified, while several C=C, C=N, and ring vibrations of the free ligand appear significantly shifted and occasionally split in the 1200–1500- cm^{-1} region. The 1469- cm^{-1} band assignable to $\nu(\text{C}(8)\text{=N}(7)) + \delta(\text{C}(8)\text{--H})$ ^{30a} is shifted to lower frequencies by about 10 cm^{-1} and the 1421- cm^{-1} band due to $\nu(\text{C}(4)\text{--N}(9)) + \nu(\text{N}(7)\text{--C}(5))$,²⁵ increases its frequency to 1432 cm^{-1} . These variations related to the five-membered ring as well as the splitting of the 1215- cm^{-1} band assignable to $\delta(\text{C}(8)\text{--H}) + \nu(\text{C}(8)\text{=N}(7))$ have been observed in the spectra of several structurally known N(7)-metalated complexes.^{30a,35} The bands centered at about 1367, 1350, and 1275 cm^{-1} in the free base spectrum assigned to the N(9)–C(8), N(7)–C(5), C(6)–N(1) stretching and C(8)–H bending vibrations exhibit major intensity and frequency changes that are also diagnostic of N(7)-metal binding.^{30d,e} This implies coordination of Ni(II) with the imidazole ring, probably through N(7), but no clear distinction between N(7) and N(9) binding site can be inferred from these data. In addition, some changes on the bands appearing at 967, 910, and 898 cm^{-1} , related to $\nu(\text{N}(3)\text{--C}(2))$ and to $\nu(\text{N}(3)\text{--C}(5)) + \delta(\text{N}(3)\text{--C}(2))$, respectively, point out that N(3) might be involved, as well, in the bonding. Again, the bridging binding mode can not be ruled out. The N(3)–N(9) and N(7)–N(3) binding modes have been identified in X-ray crystallographic studies of polymeric hypoxanthine compounds.^{5,36}

For the cytosine complex **3**, the infrared data agree with C(2)–O bonding derived from the crystal structure determination. The very strong $\nu(\text{C}(2)\text{=O})$ band²⁷ at 1664 cm^{-1} in the spectrum of the free base shifts to lower frequencies at about 1646 cm^{-1} upon complexation. This is consistent with a slight decrease of

its double-bond character [$\text{C}(2)\text{=O} = 1.263(5) \text{ \AA}$] with respect to the corresponding value in the metal free cytosine [$\text{C}(2)\text{=O} = 1.237 \text{ \AA}$].³⁷ Contrarily, in the 5'-CMP complex with direct Mn–O(2) coordination,^{6c} it was pointed out that this interaction had little effect on the carbonyl stretching band. The bands centered at about 1636, 1617, 1504, 1466, and 1366 cm^{-1} in the free ligand spectrum assigned to $\nu(\text{C=C})$, $\nu(\text{C=N})$, $\delta(\text{NH}_2)$, and ring vibrations exhibit intensity changes and shifts in their frequency as a consequence of the new charge distribution in the ring system. Other pyrimidine ring bands are masked by the absorptions of the BPh₄ group. The changes in the bands related to NH₂ bending modes are probably due to the absence of H bonding in the complex.

Modification of the $\nu(\text{Ni}\text{--N})$ band,^{38a} at 356 cm^{-1} in the starting complex, is observed in the three spectra, and the strong band at 1038 cm^{-1} assigned to $\nu(\text{C}\text{--C})/\nu(\text{C}\text{--N})$ of the ethylenediamine groups is differently affected in purine and pyrimidine compounds. In the purine complexes **1** and **2**, the strong band is shifted to 1020 cm^{-1} , but it remains in its original broad form. Contrarily, in the cytosine complex, the band is displaced to 1000 cm^{-1} and changes to a sharp form.³⁹ These results are in agreement with the cytosine complex structure and also with the considered structure for the adenine and hypoxanthine complexes.

Electronic Spectra and Magnetic Properties. The $\pi \rightarrow \pi^*$ transitions bands⁴⁰ of the purine and pyrimidine bases (200–270 nm) show several intensity changes upon metal complex formation. In contrast, the band energies are, with the exception of that for **2**, rather insensitive to metal complex formation (Table V). The noticeable shift to lower energies in the hypoxanthine bands of **2** (204 and 249 nm) is related to the presence of the monoanionic purine ligand.⁴¹

The d–d transition spectra of the three complexes are suggestive of approximately octahedral stereochemistry. Two bands are observed in the solution spectra (10^{-4} M) which may be assigned to the transitions $\nu_2, {}^3A_{2g}(F) \rightarrow {}^3T_{1g}(F)$ (545–570 nm), and $\nu_3, {}^3A_{2g}(F) \rightarrow {}^3T_{1g}(P)$ (347–356 nm). The d–d splittings in **1** and the broad character of the bands indicate the presence of low-symmetry components in the ligand field.⁴² The very weak bands appearing between ν_2 and ν_3 may correspond to singlet–triplet transitions as well as the weak band at 750 nm in the cytosine complex, although mixing of excited states via spin–orbit coupling cannot be ruled out.⁴³ Approximate Dq values calculated for the three complexes seem reasonable for MN_6 (**1**, **2**) and MN_4O_2 (**3**) chromophores.^{44,45}

(32) Lautie, A.; Novak, A. *J. Chem. Phys.* **1974**, *71*, 415.

(33) (a) De Meester, P.; Skapski, C. *J. Chem. Soc., Dalton Trans.* **1972**, 2400. (b) Sletten, E. *Acta Crystallogr.* **1969**, *B25*, 1480. (c) De Meester, P.; Skapski, C. *J. Chem. Soc. A* **1971**, 2167. (d) Terzis, A.; Beauchamp, A. L.; Rivest, R. *Inorg. Chem.* **1973**, *12*, 1166. (e) Sletten, E. *Chem. Commun.* **1967**, 1119.

(34) Vestues, P.; Sletten, E. *Inorg. Chim. Acta* **1981**, *52*, 269.

(35) Tajmir-Riahi, H. A.; Theophanides, T. *Inorg. Chim. Acta* **1983**, *80*, 223.

(36) Sletten, E. *Acta Crystallogr.* **1970**, *B26*, 1609.

(37) Voet, D.; Rich, A. *Prog. Nucleic Acid Res. Mol. Biol.* **1970**, *10*, 183.

(38) (a) Nakamoto, K. *Infrared and Raman Spectra of Inorganic and Coordination Compounds*; Wiley: New York, 1978. (b) Lever, A. B. P.; Mantovani, E. *Can. J. Chem.* **1973**, *51*, 1567.

(39) Baldwin, M. E. *J. Chem. Soc.* **1960**, 4369.

(40) Clark, L. B.; Tinoco, I. *J. Am. Chem. Soc.* **1965**, *87*, 11.

(41) (a) Mason, S. F. *J. Chem. Soc.* **1954**, 2071. (b) Brown, D. J.; Mason, S. F. *J. Chem. Soc.* **1957**, 682.

(42) Byers, W.; Lever, A. B. P.; Parish, R. V. *Inorg. Chem.* **1968**, *7*, 1835.

(43) Hart, S. M.; Boeyens, J. C. A.; Hancock, R. D. *Inorg. Chem.* **1983**, *22*, 982.

(44) Lever, A. B. P. *Inorganic Electronic Spectroscopy*; Elsevier: Amsterdam, 1984.

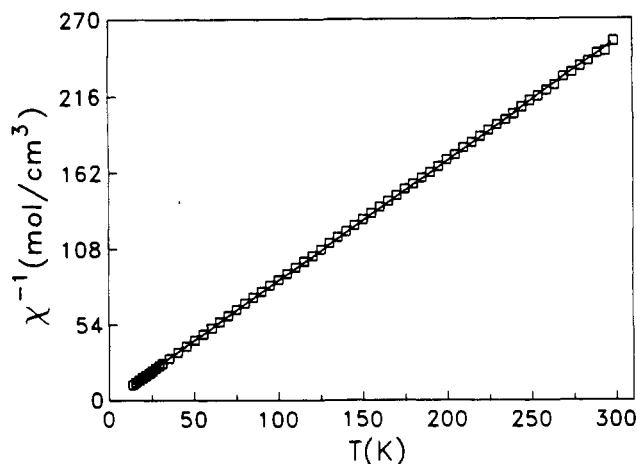


Figure 4. Reciprocal molar paramagnetic susceptibility for the $[\text{Ni}(\text{en})_2(\text{Cyt})_2](\text{BPh}_4)_2$ complex. The solid line represents the fit to a Curie-Weiss law $\chi = C/(T - \theta)$ with $C = 1.18 \pm 0.01 \text{ cm}^3 \text{ K mol}^{-1}$ and $\theta = 0.2 \pm 0.5 \text{ K}$.

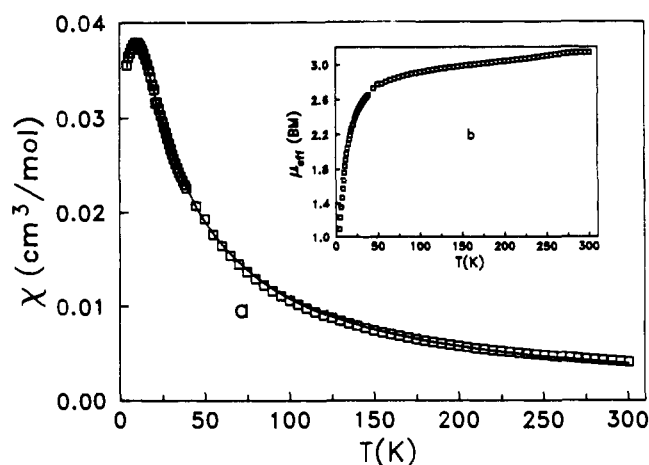


Figure 5. Temperature dependence of the molar paramagnetic susceptibility (a) and effective magnetic moment per Ni(II) ion (b) in the $[\text{Ni}(\text{en})_2(\text{Hyp})]\text{Cl} \cdot 0.5\text{CH}_3\text{OH} \cdot \text{H}_2\text{O}$ complex. The solid line in part a gives the best theoretical fit to experimental data by using eq 1 from the text with $J = -2.36 \text{ cm}^{-1}$, $g = 2.23$, and $N_\alpha = 15 \times 10^{-6} \text{ cgsu}$.

The reciprocal molar magnetic susceptibility, χ^{-1} , plotted versus temperature for the $[\text{Ni}(\text{en})_2(\text{Cyt})_2](\text{BPh}_4)_2$ complex, is shown in Figure 4. The experimental data follows a Curie-Weiss law $\chi = C/(T - \theta)$ solid line in Figure 4, with a Curie constant C of $1.18 \pm 0.01 \text{ cm}^3 \text{ K mol}^{-1}$ and a Curie temperature θ of $0.2 \pm 0.5 \text{ K}$. The effective magnetic moment μ_{eff} of $3.07 \mu_{\text{B}}$ at room temperature, which is characteristic for an octahedral Ni(II) compound,⁴⁶ remains practically constant down to 40 K and thereafter increases slightly up to $3.19 \mu_{\text{B}}$ at 14 K. The constancy of μ_{eff} over the temperature range studied, along with the small value of θ , is characteristic of a magnetically diluted system such as would be expected from the crystal structure.

On the other hand, the other two complexes $[\text{Ni}(\text{en})_2(\text{Ade})]\text{Cl}_2$ and $[\text{Ni}(\text{en})_2(\text{Hyp})]\text{Cl} \cdot 0.5\text{CH}_3\text{OH} \cdot \text{H}_2\text{O}$ have magnetic susceptibility curves that are characteristic of an antiferromagnetic exchange interaction. Figure 5 illustrates the data obtained for the hypoxanthine derivative. Upon sample cooling, χ first increases, reaching a maximum at 10 K, and then decreases. The μ_{eff} at 300 K is $3.17 \mu_{\text{B}}/\text{Ni}(\text{II})$ ion and this decreases gradually down to 50 K whereupon the μ_{eff} value decreases more rapidly with decreasing temperature down to $1.09 \mu_{\text{B}}/\text{Ni}(\text{II})$ ion at 4.2 K, a behavior that is indicative of an antiferromagnetic interaction.

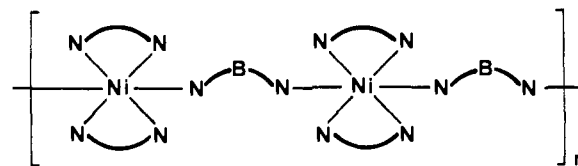


Figure 6. Chainlike model proposed for the $[\text{Ni}(\text{en})_2(\text{Hyp})]\text{Cl} \cdot 0.5\text{CH}_3\text{OH} \cdot \text{H}_2\text{O}$ and $[\text{Ni}(\text{en})_2(\text{Ade})]\text{Cl}_2$ complexes. N-B-N stands for the hypoxanthine and adenine bases.

The Curie temperature θ of $16.9 \pm 1.4 \text{ K}$ is of the same magnitude as that found in the $[\text{Ni}(\text{purine})_2(\text{H}_2\text{O})_2](\text{ClO}_4)_2$ complex, in which the most likely structure involves a linear chainlike polymeric complex.⁴⁷ In this complex, it is postulated that a single purine acts as a bridge between adjacent metal ions, such as in the established crystal structure of $[\text{Ni}(\text{purine})(\text{H}_2\text{O})_4]\text{SO}_4 \cdot 2\text{H}_2\text{O}$.³⁴ This analogy, together with the scarce solubility of these complexes in water, prompted us to fit the present experimental data by using Fisher's classical Heisenberg results⁴⁸ for infinite linear chains. Fisher's equation for magnetic susceptibility of a classical spin S chain is⁴⁸ (with inclusion of a temperature-independent term, N_α)

$$\chi = \frac{Ng^2\beta^2S(S+1)}{3kT} \frac{1-u}{1+u} + N_\alpha \quad (1)$$

where

$$u = \frac{T}{T_0} - \coth\left(\frac{T_0}{T}\right) \quad (2)$$

and

$$T_0 = \frac{2JS(S+1)}{k} \quad (3)$$

and where J is the intrachain exchange parameter. The fit obtained for $J = -2.36 \text{ cm}^{-1}$, $g = 2.23$, and $N_\alpha = 15 \times 10^{-6} \text{ cgsu}$, with an agreement factor $R = \sum[\chi_{\text{exp}}(t) - \chi_{\text{cal}}(t)]^2 / \sum[\chi_{\text{exp}}(t)]^2$ of 0.65×10^{-4} , is shown as the solid curve in Figure 5b.

In the case of the adenine derivative, the molar paramagnetic susceptibility, χ , continues to increase with decreasing temperature down to 4.2 K. The μ_{eff} per Ni(II) ion at 50 K is $3.14 \mu_{\text{B}}$ and this decreases to $2.52 \mu_{\text{B}}$ for 5 K, the Curie temperature being $\theta = 12.4 \pm 1.6 \text{ K}$, lower than that of the hypoxanthine derivative. Least-squares fitting of the data for this compound to eq 1 gives $J = -0.26 \text{ cm}^{-1}$, $g = 2.08$, and $N_\alpha = 330 \times 10^{-6} \text{ cgsu}$.

According to the results of the magnetic fittings, it is reasonable to think that the $[\text{Ni}(\text{en})_2(\text{Hyp})]\text{Cl} \cdot 0.5\text{CH}_3\text{OH} \cdot \text{H}_2\text{O}$ and $[\text{Ni}(\text{en})_2(\text{Ade})]\text{Cl}_2$ complexes have linear chainlike structures as is shown in Figure 6. This structural model is in good agreement with the spectroscopic data. However, in the case of the electronic spectra, the bands observed could be due to monomeric species resulting from the partial rupture of the linear chains in solution, and this would explain the slight solubility of these complexes.

The greater antiferromagnetic interaction exhibited by the hypoxanthine derivative may be attributed to the presence of the hypoxanthine moiety in its anionic form. If the hypoxanthine and the adenine bases in their respective complexes act as bridges among the Ni(II) ions, it is likely that the anionic base would lead to a large J value for its exchange pathway.

Acknowledgment. We are grateful to the DGICYT, Ref. PB86-0074, for financial support and to Prof. X. Tejada and Dr. A. Labarta for the use of the magnetic facilities.

Supplementary Material Available: Tables of anisotropic thermal parameters, final hydrogen coordinates, and other interatomic bond lengths and angles for the cytosine complex 3 (3 pages). Ordering information is given on any current masthead page. Additional information about magnetic measurements can be requested directly from the authors.

(45) Rosenberg, R. C.; Root, C. A.; Gray, H. B. *J. Am. Chem. Soc.* **1975**, *97*, 21. (b) Lever, A. B. P.; Paoletti, P.; Fabbri, L. *Inorg. Chem.* **1979**, *18*, 1324.

(46) Casey, A. T.; Mitra, S. In *Theory and Applications of Molecular Paramagnetism*; Boudreaux, E. A., Mulay, N., Ed.; Wiley: New York, 1976.

(47) Specia, A. N.; Mikulski, C. M.; Iaconianni, F. J.; Pytlewski, P. L.; Karayannis, N. M. *Inorg. Chem.* **1980**, *19*, 3491.

(48) Fisher, M. E. *Am. J. Phys.* **1964**, *32*, 343.